Hydrogenic impurity states in quantum dots and quantum wires

D. S. Chuu, C. M. Hsiao, and W. N. Mei*
Department of Electrophysics, National Chiao Tung University, Hsinchu, Taiwan, Republic of China
(Received 14 January 1992; revised manuscript received 24 March 1992)

The energies of hydrogenic impurity states with an impurity atom located at the center of a quantum dot and on the axis of a quantum-well wire are studied. These two systems are all assumed to have an infinite confining potential. In the case of the quantum dot, the impurity eigenfunctions are expressed in terms of Whittaker functions and Coulomb scattering functions. The calculated ground-state energy of the impurity approaches the correct limit of three-dimensional hydrogen atom as the radius of the quantum dot becomes very large. In the case of the quantum-well wire, analytical solutions can be obtained if we divide the space into a two-dimensional subspace (perpendicular to the axis of the quantum-well wire) and a one-dimensional subspace (parallel to the axis of the quantum-well wire). The calculated ground-state energy of the quantum-well wire approaches the ground-state energy of the shallow-impurity atom located on the surface as the radius of the wire becomes infinite. Variations of the state energies with the radius of the quantum dot and the quantum-well wire are obtained.

I. INTRODUCTION

In the past ten years, impurity states in various confined systems, such as quantum wells, quantum-well wires, and quantum dots, have been a subject of extensive investigations in basic and applied research.[1-29] Quasi-two-dimensional (quasi-2D) quantum wells have been widely studied and applied[1] to various semiconductor devices, such as high-electron-mobility transistors. Quasi-one-dimensional systems, such as quantum-well wires, are known to have the advantage of high mobility and suppression of carrier scattering.[2] The emission line for quantum well wires was observed[2] to be two to three times broader than that of the two-dimensional quantum wells and occurred at 6–10-meV higher binding energy.

Studies of quantum dots or quantum-well wires are very interesting problems because specific properties of these lower-dimensional structures can be easily achieved by varying the radius of the quantum dot or the quantum-well wire. An electron bound to an impurity atom located at the center of the quantum dot or on the axis of the quantum-well wire may appear to be unaffected by the boundary when the radius is very large and behaves very much like an impurity atom in the three-dimensional case. However, as the radius is reduced, spatial confinement begins to cause the kinetic energy of the electron to increase due to the uncertainty principle and eventually it may overcome the attractive potential between the electron and the impurity atom; thus the total energy may change from negative to positive at a certain radius of the confining system and finally diverges to infinity as the radius approaches zero. Moreover, the effective strength of the Coulomb interaction between the electron and the impurity atom depends on the geometric dimension of the system and is enhanced as the size of the system is reduced. Thus, in quantum-well wires or quantum dots the effective strength of the Coulomb interaction can be changed by varying the radius of the quantum-well wire or the quantum dot. Conversely, dramatic changes in the binding energies may serve as a clear signal for changes in the effective dimension of quantum-well wires or quantum dots.

Upon reduction of the geometric dimension, the confinement of electron motion becomes a pronounced effect. The physical properties of electrons in quantum-well wires or quantum dots are thus very different from those in the bulk. The impurity state in a quantum-well wire (or a quantum dot) has a spectrum composed of subbands of one- (or zero-) dimensional single-particle states. Each subband is continuous as a function of the wave vector and the energy gap between subbands is determined by the splitting of the levels in the confining system. The density of state (DOS) of electrons in each subband is proportional to $E^{1/2}$ for the bulk and is a constant for a given quantum well. The DOS is proportional to $E^{-1/2}$ for a quantum-well wire, while it behaves like a δ function for a quantum dot.

Many theoretical works have been devoted to the study of the properties of impurity states in various confining systems.[3-28] Lee and Spector[4] have calculated the binding energies for the bound states of a hydrogenic impurity placed on the axis of a cylindrical quantum-well wire of infinite confining potential. Later, Bryant[8-10] improved the model calculation by assuming a finite barrier for the confining potential with the impurity on and off the axis of the cylinder wire. The binding energies for the bound states of hydrogenic impurity in a quantum-well wire of GaAs surrounded by $Ga_{1-x}Al_xAs$ have been found to be 2–3 times larger than those in comparable two-dimensional wells.[10] In the calculation of the hydrogenic impurity states, a variational principle with a trial wave function which takes into account the confinement of the carriers in the quantum-well wire or the quantum dot was usually employed.[10-16] Zhu, Xiong, and Gu[17] used hydrogenic-effective-mass theory to study donor states in a spherical GaAs-$Ga_{1-x}Al_xAs$ quantum dot. Exact solution and quantum-level structures were obtained. In the investigation of the behavior of the hydro-

genlike impurity states in a small quantum-well wire, the effects of disorder were also taken into account.[19] Zhao *et al.*[20] studied the collective excitations of edge-state electrons in a quasi-one-dimensional quantum-well wire under a large transverse magnetic field. The plasmon modes for both intrasubband and intersubband excitations were found. Briggs and Leburton[21] employed a Monte Carlo simulation of multisubband quasi-one-dimensional quantum-well wire. In their calculation, effects of polar-optical-phonon and inelastic acoustic-phonon scattering have been included. Although many works have investigated various aspects of the electronic properties in the lower-dimensional structures as mentioned above, a full theoretical understanding of these bound states and their binding energies is still lacking.

In this paper we present a detailed formulation for the state energies of a hydrogenic impurity located at the center of a quantum dot and or a quantum-well wire. Variations of the state energies with the radius of quantum-well wires and quantum dots are presented.

II. FORMULATION

A. Quantum dot

Consider a hydrogenic impurity located at the center of a spherical dot which is confined by an infinite spherical potential well with radius a. The Hamiltonian of this system can be written as

$$H=\left[\frac{\hbar^2}{2\mu}\nabla^2-\frac{Ze^2}{\epsilon r}+V(r)\right], \tag{1}$$

where

$$V(r)=\begin{cases}0, & r<a\\ \infty, & r>a\end{cases}$$

and μ, ϵ, and Z are the effective mass, dielectric constant, and core charge. $V(r)$ is the confining potential. The Schrödinger equation for H in spherical coordinates (r,θ,φ) for $r<a$ can be written as

$$-\frac{\hbar^2}{2\mu}\left[\frac{\partial^2}{\partial r^2}+\frac{2\partial^2}{r_{\partial r}}+\frac{1}{r^2\sin\theta}\frac{\partial}{\partial\theta}\left[\sin\theta\frac{\partial}{\partial\theta}\right]+\frac{1}{r^2\sin^2}\frac{\partial^2}{\theta\partial\varphi^2}\right]\Psi-\frac{Ze^2}{\epsilon r}\Psi=E\Psi \tag{2}$$

and $\Psi(r=a,\theta,\varphi)=0$ because the potential is infinite for $r>a$. $\Psi(r,\theta,\varphi)$ may be separated into the product $R(r)\Theta(\theta)\psi(\varphi)$, as in the case of the hydrogen atom, $\Theta(\theta)$ is the associated Legendre polynomial, and $\psi(\varphi)=e^{im\varphi}$, $m=0,\pm1,\pm2\ldots$. The differential equation for the radial part $R(r)$ can be obtained as follows:

$$-\frac{\hbar^2}{2\mu}\left[\frac{\partial^2}{\partial r^2}+\frac{2}{r}\frac{\partial^2}{\partial r}-\frac{L(L+1)}{r^2}\right]R(r)-\frac{Ze^2}{\epsilon r}R(r)=ER(r), \tag{3}$$

with $R(a)=0$. Since the motion of the electron is confined inside the dot, the existence of positive bound states is possible. Therefore, one can study solutions of the Schrödinger equation in two regions. (1) For $E<0$, the solutions can be expressed in terms of Whittaker functions. (2) For $E>0$, the solutions can be expressed in terms of the Coulomb-scattering wave functions, as can be seen in the following:

(1) Negative-energy region, $E<0$. We first set $\xi=\alpha,r$, with $\alpha^2=-8\mu E/\hbar^2>0$. Then Eq. (3) becomes

$$\frac{\partial^2R}{\partial\xi^2}+\frac{2}{\xi}\frac{\partial R}{\partial\xi}+\left[-\frac{1}{4}+\frac{\lambda}{\xi}-\frac{L(L+1)}{\xi^2}\right]R=0, \tag{4}$$

where $\lambda=2\mu Ze^2/\epsilon\hbar^2\alpha$ and $R(\alpha a)=0$. If we further write $R(\xi)=\xi^{-1}F(\xi)$, then Eq. (3) can be rewritten as

$$F''(\xi)+\left[-\frac{1}{4}+\frac{\lambda}{\xi}+\frac{\frac{1}{4}-(L+\frac{1}{2})^2}{\xi^2}\right]F(\xi)=0. \tag{5}$$

Equation (5) is the Whittaker equation[30] with the solutions as

$$F_{\lambda,L}(\xi)=e^{-\xi/2}\xi^{L+1}\Phi(L+1-\lambda,2L+2,\xi), \tag{6a}$$

or

$$F_{\lambda,-L}(\xi)=e^{-\xi/2}\xi^{-L+1}\times\Phi(-L+1-\lambda,-2L+2,\xi), \tag{6b}$$

where Φ is the confluent hypergeometric function

$$\Phi(a,b,x)=1+\frac{a}{b}\frac{x}{1}+\frac{a(a+1)1}{b(b+1)2!}x^2+\cdots+\frac{a(a+1)(a+2)\cdots(a+k)1}{b(b+1)(b+2)\cdots(b+k)(k+1)!}\times x^{k+1}+\cdots. \tag{6c}$$

Hence, $R(\xi)$ of Eq. (4) can be expressed as

$$R(\xi)=\xi^{-1}F_{\lambda,L}(\xi)=e^{-\xi/2}\xi^{L}\Phi(L+1-\lambda,2L+2,\xi), \tag{7a}$$

or

$$R(\xi)=\xi^{-1}F_{\lambda,-L}(\xi)=e^{-\xi/2}\xi^{-L}\Phi(-L+1-\lambda,-2L+2,\xi). \tag{7b}$$

Since we require the wave function to be finite everywhere, the wave function must be in the form of Eq. (7a) for $L>0$ or Eq. (7b) for $L<0$, i.e.,

$$R(\xi)=e^{-\xi/2}\xi^{|L|}\Phi(|L|+1-\lambda,2|L+2,\xi). \tag{7c}$$

Because L represents the total angular momentum, which is always positive, $|L|$ can be replaced by L in the above solution. The value of λ can be determined from the boundary condition $R(\xi=\alpha a)=0$, which is equivalent to setting

$$\Phi(L+1-\lambda,2L+2,\alpha a)=0 \tag{8}$$

and the total energy of the system may be given as

$$E=-\frac{\mu Z^2e^4}{2\epsilon^2\hbar^2}\frac{1}{\lambda^2}. \tag{9}$$

It is easy to prove that Φ is an even function of λ; thus, we need only consider the case where $\lambda > 0$.

(2) Positive-energy region, $E > 0$. First set $\xi = \alpha r$, where $\alpha^2 = -2\mu E/\hbar^2 < 0$; then Eq. (3) becomes

$$\frac{\partial^2 R}{\partial \xi^2} + \frac{2}{\xi}\frac{\partial R}{\partial \xi} + \left[1 - \frac{2\eta}{\xi} - \frac{L(L+1)}{\xi^2}\right] R = 0 , \quad (10)$$

where $n = -\mu Z e^2/\epsilon\hbar^2\alpha$ and $R(\alpha a) = 0$. If we further set $R(\xi) = \xi^{-1}F(\xi)$, then Eq. (10) becomes

$$F''(\xi) + \left[1 - \frac{2\eta}{\xi} - \frac{L(L+1)}{\xi^2}\right] F(\xi) = 0 . \quad (11)$$

Equation (11) is a Coulomb equation.[31] The solutions of Eq. (11) are $F_{\eta,L}(\xi)$ and $G_{\eta,L}(\xi)$:

$$F_{\eta,L}(\xi) = e^{-i\xi}\xi^{L+1}\Phi(L+1-i\eta, 2L+2, 2i\xi) , \quad (12a)$$

$$G_{\eta,L}(\xi) = F_L(\eta,\xi)\left[\ln(2\xi) + \frac{q_L(\eta)}{p_L(\eta)}\right] + \theta_L(\eta,\xi) , \quad (12b)$$

where Φ is the confluent hypergeometric function as shown in Eq. (6c). $F_{\eta,L}(\xi)$ can be expressed in another form as

$$F_{\eta,L}(\xi) = \xi^{L+1}\Phi_L(\eta,\xi) , \quad (12c)$$

where $\Phi_L(\eta,\xi)$ is defined as

$$\Phi_L(\eta,\xi) = \sum_{k=L+1}^{\infty} A_k^L(\eta)\xi^{k-L-1} , \quad (12d)$$

with $A_{L+1}^L = 1$,

$$A_{L+2}^L(\eta) = \eta/(L+1) ,$$

and

$$(k+L(k-L-1)A_k^L = 2\eta A_{k-1}^L(\eta) - A_{k-2}^L(\eta)$$

for $k > L+2$. Since $G_{\eta,L}(\xi)$ is singular at $\xi = 0$, only $F_{\eta,L}(\xi)$ is used as the solution of the system. Hence, $R(\xi)$ of Eq. (10) may be written as

$$R(\xi) = \xi^L\Phi_L(\eta,\xi) . \quad (13)$$

The value of η can be determined from the boundary condition

$$\Phi_L\left[\eta, \frac{-\mu Z e^2}{\epsilon\hbar^2\eta}a\right] = 0 , \quad (14)$$

and the total energy of the system may be given as

$$E = \frac{\mu Z^2 e^4}{2\epsilon^2\hbar^2}\frac{1}{\eta^2} . \quad (15)$$

Since $\Phi_L(\eta,\xi)$ is an even function of η, we only need to consider $\eta > 0$.

(3) The turning point in energy from $E > 0$ to $E < 0$. The turning point for the bound-state energy changing from positive to negative can be obtained by setting $E = 0$ in Eq. (3):

$$-\frac{\hbar^2}{2\mu}\left[\frac{\partial^2}{\partial r^2} + \frac{2}{r}\frac{\partial}{\partial r} - \frac{L(L+1)}{r^2}\right] R(r) - \frac{Ze^2}{\epsilon r}R(r) = 0 . \quad (16)$$

Comparing with the modified Bessel equation

$$x^2\frac{\partial^2 y}{\partial x^2} + (1-2s)x\frac{\partial y}{\partial x} + [(s^2-\gamma^2\alpha^2) + \alpha^2\gamma^2x^2]y = 0 , \quad (17)$$

we obtain $s = \frac{1}{2}$, $\gamma = \frac{1}{2}$, $\alpha^2 = (8mZe^2)/(\epsilon\hbar^2)$, and $\alpha^2 = (2L+1)^2$. Thus, the radial function for $L = 0$, which is finite as $r \to 0$, can be written as

$$R_0(r) = r^{-1/2}J_1\left[\left[\frac{8\mu Z e^2}{\epsilon\hbar^2}\right]^{1/2} r^{1/2}\right] . \quad (18)$$

To satisfy the boundary condition $R_0(a) = 0$, we require that

$$(8\mu Z e^2/\epsilon\hbar^2)a = x_i^2 ,$$

where x_i are roots of the Bessel function J_1. The radial function for $L = 1$ can be written as

$$R_1(r) = r^{-1/2}J_3\left[\left[\frac{8\mu Z e^2}{\epsilon\hbar^2}\right]^{1/2} r^{1/2}\right] . \quad (19)$$

The boundary condition $R_1(a) = 0$ yields

$$8\mu Z e^2/\epsilon\hbar^2)a = y_i^2 ,$$

where y_i are the roots of the Bessel function J_3. After substituting the values of x_i and y_i we can obtain the turning points. For example, 1s-state energy becomes positive when the radius is less than $1.8325a_0$ and 2p-state energy becomes positive when the radius is less than $5.088\,31a_0$, where a_0 is the Bohr radius. From the above discussion, one can also note that the core charge and effective mass will effect the value of the turning point and a larger effective mass or core charge will yield a smaller turning point of the energy.

B. Quantum wire

Consider now an impurity located on the axis of an infinitely high cylindrical quantum well with radius d. The Hamiltonian for this system can be expressed as

$$H = -\frac{\hbar^2}{2m_t}\left[\frac{\partial^2}{\partial x^2} + \frac{\partial^2}{\partial y^2}\right] - \frac{\hbar^2\partial^2}{2m_l\partial z^2} - \frac{Ze^2}{\epsilon r} + V(\rho) , \quad (20a)$$

where

$$V(\rho) = \begin{cases} 0, & \rho \le d \\ \infty, & \rho > d \end{cases}$$

and $r = (x^2+y^2+z^2)^{1/2}$, $\rho = (x^2+y^2)^{1/2}$; m_t and m_l are the transverse mass and longitudinal mass of the electron inside the well; ϵ is the dielectric constant of the wire material; and Ze is the core charge. The axis of the wire is

along the z direction. To solve the Schrödinger equation for the Hamiltonian defined in Eq. (20a), we first perform a coordinate transformation:

$$x=x',\ y=y',\ z=(m_t/m_l)^{1/2}z' .$$

The Hamiltonian in Eq. (20a) then becomes

$$H=-\frac{\hbar^2}{2m_t}\left[\frac{\partial^2}{\partial x'^2}+\frac{\partial^2}{\partial y'^2}+\frac{\partial^2}{\partial z'^2}\right]-\frac{Ze^2}{\epsilon r'}+V(\rho') . \tag{20b}$$

Here, $r'=(x'^2+y'^2+z'^2)^{1/2}$ and $\rho'=\rho=(x'^2+y'^2)^{1/2}$. For convenience, we shall drop the prime for the coordinate variables from now on. Now we rewrite the Hamiltonian in the following form:

$$H=H_{01}(\beta)+H_{02}(\alpha)+H'(\alpha,\beta) , \tag{20c}$$

where

$$H_{01}(\beta)=-\frac{\hbar^2}{2m_t}\frac{\partial^2}{\partial z^2}-\frac{\beta e^2}{\epsilon z} , \tag{20d}$$

$$H_{02}(\alpha)=-\frac{\hbar^2}{2m_t}\left[\frac{\partial^2}{\partial x^2}+\frac{\partial^2}{\partial y^2}\right]-\frac{\alpha e^2}{\epsilon\rho}+V(\rho) , \tag{20e}$$

$$H'(\alpha,\beta)=\frac{\beta e^2}{\epsilon z}+\frac{\alpha e^2}{\epsilon\rho}-\frac{ze^2}{\epsilon r} , \tag{20f}$$

$$V(\rho)=\begin{cases}0, & \rho\le d\\ \infty, & \rho>d ,\end{cases}$$

and α and β are the unknown parameters which are to be treated as variational parameters and can be determined later. Decomposing H into H_{01} and H_{02} in Eq. (20c) is equivalent to dividing the space into two-dimensional (perpendicular to the axis) and one-dimensional (parallel to the axis) subspaces. Let us take

$$H_0(\alpha,\beta)=H_{01}(\beta)+H_{02}(\alpha)$$

as the unperturbed Hamiltonian and regard $H'(\alpha,\beta)$ as the perturbation term (which can be adjusted as a small term by varying the parameters α and β). The unperturbed ground-state wave function and the unperturbed ground-state energy for the Hamiltonian $H_0(\alpha,\beta)$ may be written as

$$\Psi_g^{(0)}(r;\alpha,\beta)=\Psi_g^{(01)}(z;\beta)\Psi_g^{(02)}(x,y;\alpha) , \tag{21a}$$

$$E_g^{(0)}(\alpha,\beta)=E_g^{(01)}(\beta)+E_g^{(02)}(\alpha) , \tag{21b}$$

respectively, where $\Psi_g^{(01)}(z;\beta)$ is the ground-state wave function of the 1D hydrogen atom (H_{01}), and $\Psi_g^{(02)}(x,y;\alpha)$ is the ground-state wave function of the 2D hydrogen atom in a circular well (H_{02}). For the 1D hydrogen atom, the eigenfunction and eigenvalue of the ground state may be given as

$$\Psi_g^{(01)}(z;\beta)=\sqrt{2}\omega^{3/2}|z|\exp(-\omega|z|) , \tag{22a}$$

$$E_g^{(01)}(\beta)=-\frac{m_t e^4}{\epsilon\hbar^2}\beta^2 , \tag{22b}$$

where $\omega=(2m_t e^2/\epsilon\hbar^2)\beta$. The Hamiltonian in Eq. (20e) represents a quantum-circle system in which a 2D hydrogenic impurity is located at the center of an infinite circular well. The solutions for this quantum-circle problem can be obtained in a similar way as discussed in the preceding section. The eigenfunctions for the quantum-circle system may be divided into two cases.

(1) For $E<0$,

$$\Psi_g^{(02)}(x,y;\alpha)=e^{-1/2\xi}\xi^{|m|+1/2}\times\Phi(|m|+1-\lambda,2|m|+2,\xi) ; \tag{23a}$$

(2) for $E>0$,

$$\Psi_g^{(02)}(x,y;\alpha)=\xi^m\Phi_{m-1/2}(\eta,\xi) , \tag{23b}$$

where $\Phi_{m-1/2}(\eta,\xi)$ is defined in Eq. (12d). The turning point for the energy from $E>0$ to $E<0$ in the quantum-circle system may be determined, as in the case of the quantum dot, by setting

$$d^{-1/2}J_0\left[\left[\frac{8\mu Ze^2}{\epsilon\hbar^2}\right]^{1/2}d^{1/2}\right]=0 \quad \text{for } m=0 ,$$

and

$$d^{-1/2}J_2\left[\left[\frac{8\mu Ze^2}{\epsilon\hbar^2}\right]^{1/2}d^{1/2}\right]=0 \quad \text{for } m=1 .$$

The requirement that $\Psi_g^{(02)}(x,y;\alpha)=0$ at boundary of the circle implies the following:

(1) For $E<0$,

$$\Phi(|m|+1-\lambda,2|m|+2,\alpha d)=0 . \tag{23c}$$

(2) For $E>0$,

$$\Phi_{m-1/2}(\eta,\alpha d)=0 . \tag{23d}$$

The eigenvalues may then be given as

$$E_g^{(02)}(\alpha)=-\frac{\mu Z^2e^4}{2\epsilon^2\hbar^2}\frac{1}{\lambda^2} . \tag{23e}$$

The first-order energy correction can now be obtained as

$$\begin{aligned}\Delta E_g^{(1)}(\alpha,\beta)&=\langle\Psi_g^{(0)}(r;\alpha,\beta)|H'(\alpha,\beta)|\Psi_g^{(0)}(r;\alpha,\beta)\rangle\\&=\langle\Psi_g^{(02)}(x,y;\alpha)\left|\frac{\alpha e^2}{\epsilon\rho}\right|\Psi_g^{(02)}(x,y;\alpha)\rangle\\&\quad+\langle\Psi_g^{(01)}(z;\beta)\left|\frac{\beta e^2}{\epsilon z}\right|\Psi_g^{(01)}(z;\beta)\rangle\\&\quad-\langle\Psi_g^{(0)}(r;\alpha,\beta)\left|\frac{Ze^2}{\epsilon r}\right|\Psi_g^{(0)}(r;\alpha,\beta)\rangle .\end{aligned} \tag{23f}$$

The second term on the right-hand side (rhs) in the above equation can be integrated analytically to give

$$\left\langle\Psi_g^{(01)}(z;\beta)\left|\frac{\beta e^2}{\epsilon z}\right|\Psi_g^{(01)}(z;\beta)\right\rangle=\frac{m_t e^4}{\epsilon^2\hbar^2}\beta^2 . \tag{23g}$$

The third term of Eq. (23f) can be reduced to a one-variable integral and readily integrated over z to give

$$\int R^2(\rho)\rho\, d\rho 2\int_0^\infty dz \frac{(\sqrt{2}\omega^{3/2})^2 z^2 e^{-2\omega z}}{[x^2+y^2+(m_t/m_l)z^2]^{1/2}}$$

$$=(2\omega'^{3/2})^2\int_0^\infty R^2(\rho)\frac{\pi\rho^3}{2}\,d\rho\left\{\tfrac{1}{2}[N_{\nu-1}(2\omega'\rho)-N_{\nu+1}(2\omega'\rho)]\right.$$

$$\left.-\tfrac{1}{2}[H_{\nu-1}(2\omega'\rho)-H_{\nu+1}(2\omega'\rho)+\pi^{-1/2}(\rho/2)^\nu[\Gamma(\nu+\tfrac{3}{2})]^{-1}]\right\}, \tag{23h}$$

where $\omega'=(m_l/m_t)\omega$; $H_\nu(\rho)$ and $N_\nu(\rho)$ are the Struve functions and Neumann functions, respectively. Using Eqs. (23g) and (23h), and after performing some numerical integrations, the total-state energy, up to the first-order correction, may in principle be obtained as[32]

$$E_g(\alpha,\beta)=E_g^{(01)}(\beta)+E_g^{(02)}(\alpha)+\Delta E_g^{(1)}(\alpha,\beta)\ , \tag{23i}$$

which contains parameters of α and β. The optimum values of α and β can be determined by noting that the total Hamiltonian H in Eq. (20b) or (20c) does not contain the parameters α or β so that the exact eigenvalues of H should be independent of α and β. However, in most cases occurring in practice, one cannot obtain the exact eigenvalues of the Hamiltonian H, and only an approximate solution is attainable. Thus, in the perturbation treatment, the values of α and β can be chosen so that the approximate total-energy eigenvalue in Eq. (23i) should be least sensitive to the parameters α and β. This is equivalent to the following conditions:

$$\frac{\partial E_n}{\partial\alpha}=0 \text{ and } \frac{\partial E_n}{\partial\beta}=0\ . \tag{24}$$

By using Eq. (24), the values of α and β can be determined. Thus, the total-state energy of the quantum wire can be obtained.

III. RESULTS AND DISCUSSIONS

Figure 1 shows the variation of the calculated $1s$ $(n=1,L=0)$, $2s$ $(n=2,L=0)$, and $2p$ $(n=2,L=1)$ -state energies of a hydrogenic impurity located at the center of a quantum dot for the given dot radius. The energy is expressed in terms of the effective Rydberg $\mathcal{R}^*=e^2/(2\epsilon a_0^*)$, where $\epsilon=\kappa\epsilon_0$, ϵ_0 is the dielectric constant of free space, and the radius is expressed in terms of the effective Bohr radius $(a_0^*=\epsilon^2/(\mu e^2)$, where $\mu=a_t m_0$, with a_t the ratio of the effective mass of electrons in different material to the bare electron mass. In the calculation, the m_0 and ϵ_0 are assumed to be the free-electron mass and dielectric constant of free space. One can see from the figure that the energy of the $1s$ state becomes negative when the dot radius is larger than $1.833a_0^*$ and approaches $1\mathcal{R}^*$, which is the energy of the $n=1$ state for the free-space hydrogen atom. The energy of the $2s$ state becomes negative as the dot radius becomes larger than $6.125a_0^*$. As the radius r becomes larger than $15a_0^*$, the energy of the $2s$ state in the quantum dot approaches the value $0.25\mathcal{R}^*$ of the $2s$ state in the free space. A similar situation can be observed in the case of the $2p$ state. The $2p$ state of the spherical dot has positive energy as the radius becomes smaller than $5.088a_0^*$. These two states are degenerate in the free hydrogen atom and split from each other as the radius of the dot becomes smaller than $8a_0^*$. While the radius of the dot is larger than $10a_0^*$, they become almost degenerate and approach $0.25\mathcal{R}^*$, which is the energy of the $n=2$ state for the free-space hydrogen atom. One can also note that as the radius of the quantum dot decreases, the state energy increases. Furthermore, the energy increment for the excited state is much more pronounced than that of the ground state. As the radius r approaches zero, the state energy increases infinitely.

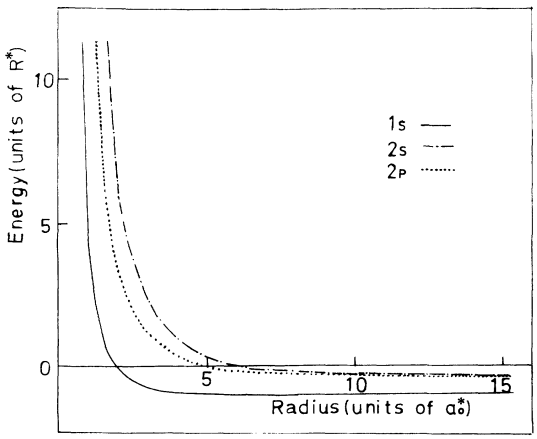

FIG. 1. $1s$-, $2s$-, and $2p$-state energies of a hydrogenic impurity located at the center of a confining sphere as a function of the radius of the confining sphere. $\mathcal{R}^*$ and a_0^* are the effective rydberg energy and the effective Bohr radius.

The binding energy E_b of the hydrogenic impurity is defined as the energy difference between the ground-state energy of the spherical-well system without the impurity and the ground-state energy of the spherical-well system with the impurity, i.e.,

$$E_b=E_{10}-E_0\ , \tag{25}$$

where E_{10} is the ground-state energy of the spherical well without the impurity and E_0 is the ground-state energy with the impurity inside the well. Figure 2 presents the E_b, E_0, and E_{10} as a function of the dot radius r. Since E_{10} is proportional to the reciprocal of the square of the dot radius, one can see that E_{10} is large except when the well width is very large. The corresponding binding energy of the Coulomb potential is proportional to the reciprocal of the radius of dot. One can note that E_b approaches a large value as r becomes very small, since the

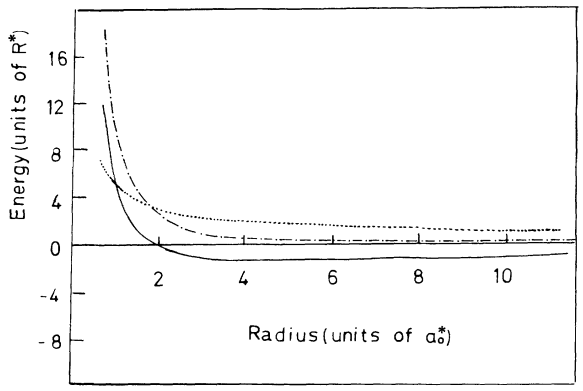

FIG. 2. The 1s-state energy (solid line), binding energy (dotted line), and kinetic energy (i.e., without the impurity, broken line) of the hydrogenic impurity located at the center of a confining sphere as the functions of the radius of a confining sphere.

electron is pushed toward the center of the spherical well by the confining potential as r approaches zero. Chu, Xiong, and Gu[17] performed a hydrogenic-effective-mass theory to calculate donor-state energies in a spherical quantum dot. To compare their result with ours, compare Fig. 1 of Ref. 17 with the broken curves of our Fig. 2. For an infinite-potential well, the ground-state energy without the impurity obtained by Chu, Xiong, and Gu is around $2.5\mathcal{R}^*$ $1.5\mathcal{R}^*$, $1.0\mathcal{R}^*$, and $0.8\mathcal{R}^*$ for a dot radius of $2a_0^*$, $2.5a_0^*$, $3a_0^*$, and $4a_0^*$, respectively. These results agree completely with our corresponding values shown in Fig. 2. To compare the ground-state binding energy for both works, one notes that the results for $V_0=\infty$ do not differ much from $V_0=80\mathcal{R}^*$ or $40\mathcal{R}^*$ for a dot radius larger than $2a_0^*$ in the work of Chu *et al.* Therefore, we may compare the results shown in Fig. 2 of Ref. 17 with the dotted curve of our Fig. 2. For example, one can see our calculated binding energy is around $2.6\mathcal{R}^*$ and $2.0\mathcal{R}^*$ for a dot radius of $2.0a_0^*$ and $3.0a_0^*$, which are in very good agreement with those obtained by Chu, Xiong, and Gu.[17] The same degree of agreement exists between our first excited state and that of Chu, Xiong, and Gu. From Figs. 1 and 2 of Ref. 17, one may easily find the excited-state energy without the impurity and the excited-state binding energy of the quantum dot. The difference between these two values yields the excited-state energy of the impurity located inside the dot. The excited-state energy of Chu, Xiong, and Gu can be obtained easily as $\sim 3.5\mathcal{R}^*$, $1.9\mathcal{R}^*$, and $1.3\mathcal{R}^*$ for a dot radius of $2a_0^*$, $2.5a_0^*$, and $3.0a_0^*$, respectively. These values are in good agreement with ours shown in the dotted curve of Fig. 1. Consider now a donor located at the center of a GaAs quantum dot. From our Fig. 2, one obtains the ground-state binding energy $E_b \sim 4.6\mathcal{R}^* = 24.4$ meV for the dot radius $R = 1a_0^*$ ($E_b = 1\mathcal{R}^* = 5.3$ meV for $R=\infty$). Ferreira da Silva[19] calculated the impurity states in a quantum-well wire of GaAs-$Ga_{1-x}Al_xAs$. They obtained the ground-state binding energy $E_b \sim 24$ meV for a wire radius of $1a_0^*$. The fact that the ground-state-impurity binding energy of a quantum dot is almost equal to that of a quantum-well wire reflects the fact that the geometrical difference becomes less important as the radius of the dot or wire becomes equal to the radius of the impurity atom.

Figure 3 presents the ground-state energies of an impurity atom located in GaAs and InAs quantum dots. The values of a_t and κ are $a_t=0.067$ and $\kappa=13.13$ for GaAs, and $a_t=0.023$ and $\kappa=14.6$ for InAs. From Fig. 3, one can see that our calculated ground-state energies of an impurity located in GaAs and InAs quantum dots for a very large radius of the confining system approach the correct limits 5.3 and 1.47 meV for the bulk GaAs and InAs semiconductors.

In the case of the quantum-well wire, instead of spherical symmetry, there is cylindrical symmetry. Figure 4 shows the ground-state energy of a hydrogenic impurity located on the axis of a cylindrical wire as a function of the wire radius. As the radius becomes very large, the impurity should behave like a free hydrogen atom with the ground-state energy of 1 Ry. However, our result shows that for larger radii, our calculated energy approaches 0.22 Ry, not 1 Ry. The inconsistency is due to the dividing of the space into two orthogonal subspaces. The 1D subspace (the one-dimensional hydrogen atom) requires that the electron wave function vanish at position $z=0$, while in the real case the electron wave function should vanish at the wire surface. This means that the method of dividing the space into 1D and 2D subspaces forces the creation of an additional node at $z=0$ plane. This is equivalent to saying that we considered a half-cylindrical wire. Thus, as the radius of the half-cylindrical wire becomes very large, our ground-state energy should approach the ground-state energy of a surface-impurity system. In the surface-impurity case, the lowest state is the $2P_0$ state of the free hydrogen atom due to the surface selection rule. This explains why our ground-state energy for the quantum wire is 0.22 Ry in-

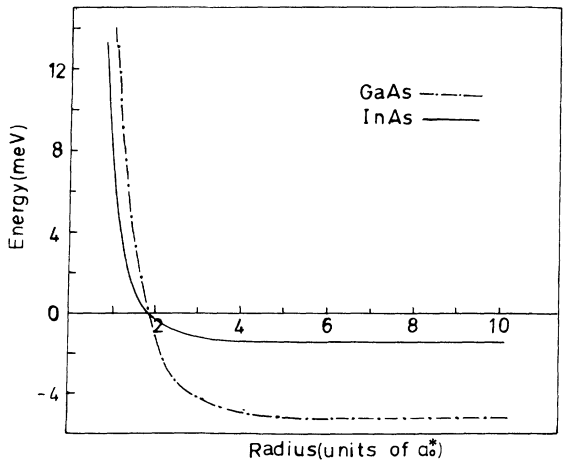

FIG. 3. The 1s-state ($L=0, n=1$) energy (in meV) of a hydrogenic impurity located at the center of semiconductor GaAs (dashed line) dot and InAs (solid line) dot as a function of the radius of the dot. a_0^* is the effective Bohr radius.

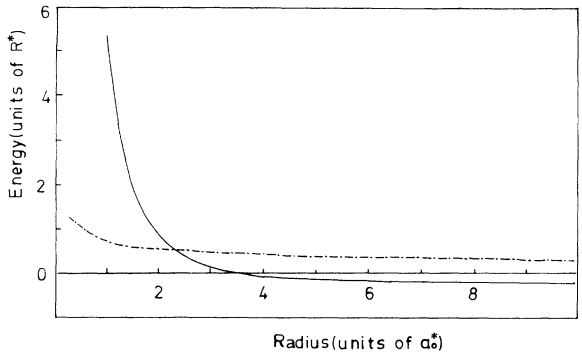

FIG. 4. The ground-state energy (solid line) and the binding energy (broken line) of a hydrogenic impurity located at the axis of a cylindrical wire as a function of the radius of the wire. $\mathcal{R}^*$ and a_0^* are the effective rydberg and the effective Bohr radius.

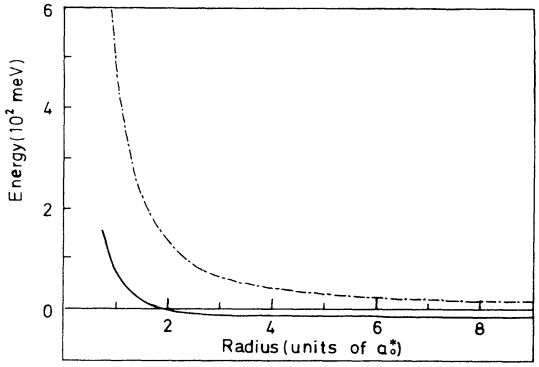

FIG. 5. The ground-state energy (in meV, solid line) and the binding energy (in meV, broken line) of a hydrogenic impurity located at the axis of a silicon cylindrical wire as a function of the radius of the wire. a_0^* is the effective Bohr radius.

stead of 1 Ry. Figure 5 shows the ground-state energy of a hydrogenic impurity located at the axis of a Si quantum wire. When the radius is very large, our calculated ground-state energy approaches the ground-state energy 10.7 meV of the surface impurity[33] of a Si semiconductor. On the contrary, the binding energies for the Si bulk semiconductor is around 28.6 meV. Bryant[10] used a variational trial wave function to calculate the binding energy of a hydrogenic impurity placed on the axis of a cylindrical quantum-well wire. He found a set of even and odd z-parity states. The binding energy of the lowest odd z parity state is lower than that of the lowest even z parity state. When the wire radius becomes very small, Bryant found that the binding energy of the lowest even z-parity state approaches 1 Ry. To compare our quantum wire shown in Fig. 4 with those of Bryant,[10] one should note that our results are similar to the odd z-parity case of Bryant because our wave function vanishes at $z=0$, which is equivalent to the case of the odd z-parity wave functions of Bryant.[10] The binding energies of the lowest even z-parity state for GaAs wire in the work of Bryant (Fig. 2 of Ref. 10) are around $5.0\mathcal{R}^*$, $3.4\mathcal{R}^*$, $2.2\mathcal{R}^*$, and $1.9\mathcal{R}^*$ ($1\mathcal{R}^*=5.3$ meV) while the binding energies of the lowest odd z-parity state are around $1.0\mathcal{R}^*$, $0.7\mathcal{R}^*$, $0.6\mathcal{R}^*$, $0.55\mathcal{R}^*$, and $0.4\mathcal{R}^*$ for the wire radius equals to $0.5a_0^*$, $1.0a_0^*$, $1.5a_0^*$, $2.0a_0^*$, and $3.0a_0^*$ ($1a_0^* \sim 100$ Å $\sim 200a_0^*$). Our corresponding results shown in Fig. 4 are around $1.1\mathcal{R}^*$, $0.75\mathcal{R}^*$, $0.65\mathcal{R}^*$, $0.59\mathcal{R}^*$, and $0.5\mathcal{R}^*$ for the wire radii equal to $0.5a_0^*$, $1.0a_0^*$, $1.5a_0^*$, $2.0a_0^*$, and $3.0a_0^*$. Therefore, our results agree very reasonably with those of the lowest odd z-parity state.

IV. CONCLUSION

We obtained the analytical solutions for the state energies of an impurity located inside a quantum dot and a quantum wire. A method of dividing the space into a one-dimensional subspace and a two-dimensional subspace has been employed to solve the impurity-state energies for a quantum wire. Whittaker functions and the scattering Coulomb wave functions are used in the case of quantum dots. It is found that as the radius of the quantum dot or the quantum-well wire becomes very large, the eigenenergies approach the corresponding state energies of the free-space hydrogen atom and become positive when the radius of the dot or wire is small. Although the present method has only been applied to infinite-confining-potential systems, when the confining potential is finite, one may employ an approximate method[34] for the finite well or use direct numerical calculation.

ACKNOWLEDGMENT

This work was supported by National Science Council, Taiwan, Republic of China.

*On leave from University of Nebraska, Omaha, Nebraska.

[1]R. Dingle, H. L. Störmer, A. C. Goassard, and W. Wiegmann, Appl. Phys. Lett. **33**, 665 (1978).
[2]H. Sakaki, Jpn. J. Appl. Phys. **19**, L735 (1980); P. M. Petroff, A. C. Gossard, R. A. Loan, and W. Wiemann, Appl. Phys. Lett. **41**, 645 (1982).
[3]P. F. Yuh and K. L. Wang, Appl. Phys. Lett. **49**, 1738 (1986).
[4]J. Lee and H. N. Spector, J. Appl. Phys. **54**, 3921 (1983); **57**, 366 (1985).
[5]V. K. Arora, Phys. Rev. B **23**, 5611 (1981).
[6]M. A. Reed, J. N. Aggarwal, R. J. Matyi, T. M. Moore, and A. E. Wetsel, Phys. Rev. Lett. **60**, 535 (1988).
[7]Ch. Sikorski and U. Merkt, Phys. Rev. Lett. **62**, 2164 (1989).
[8]G. W. Bryant, Phys. Rev. B **37**, 8763 (1988).
[9]G. W. Bryant, Phys. Rev. B **31**, 7812 (1985).
[10]G. W. Bryant, Phys. Rev. B **29**, 6632 (1984).
[11]J. W. Brown and H. N. Spector, J. Appl. Phys. **59**, 1179 (1986).
[12]E. A. de Andrada e Silva, I. C. da Cunha Lima, and A. Ferreira da Silva, Phys. Rev. B **37**, 8537 (1988).
[13]F. A. P. Osorio, M. H. Degani, and O. Hipolito, Phys. Rev. B **37**, 1402 (1988).
[14]M H. Degani and O. Hipolito, Phys. Rev. B **35**, 9345 (1987).
[15]J. W. Brown and H. N. Spector, Phys. Rev. B **35**, 3009 (1987).

[16]T. Kodama, Y. Osaka, and M. Yamanishi, Jpn. J. Appl. Phys. **24**, 1370 (1985).
[17]J. L. Zhu, J. J. Xiong, and B. L. Gu, Phys. Rev. B **41**, 6001 (1990).
[18]A. D'Andrea and R. Del Sole, Solid State Commum. **74**, 1121 (1990).
[19]A. Ferreira da Silva, Phys. Rev. B **41**, 1684 (1990).
[20]H. L. Zhao, Y. Zhu, L. Wag, and S. Feng, Phys. Lett. A **142**, 36 (1989).
[21]S. Briggs and J. P. Leburton, Phys. Rev. B **38**, 8163 (1988).
[22]A. Gold and A. Ghazali, Phys. Rev. B **41**, 7626 (1990).
[23]Y. Z. Hu, S. W. Koch, and D. B. Tra Thoai, Mod. Phys. Lett. B **4**, 1009 (1990).
[24]Y. Zhu and S. Zhou, J. Phys. A **21**, 1361 (1988).
[25]L. Banyai, I. Galbraith, C. Ell, and H. Haug, Phys. Rev. B **36**, 6099 (1987).
[26]T. Kodama and Y. Osaka, Jpn. J. Appl. Phys. **25**, 1875 (1986).
[27]W. Y. Lai and S. Das Sarma, Surf. Sci. **170**, 43 (1986).
[28]K. B. Wong, M. Jaros and J. P. Hagon, Phys. Rev. B **35**, 2463 (1987).
[29]J. Cibert, P. M. Petroff, G. J. Dolan, D. J. Werder, S. J. Pearton, A. C. Gossard, and J. H. English, Superlatt. Microstruct. **3**, 35 (1987).
[30]A. Jeffrey, *Table of Integrals, Series, and Products* (Academic, New York, 1980), p. 1059.
[31]*Handbook of Mathematical Function With Formulas, Graphs, and Mathematical Tables,* Natl. Bur. Stand. Appl. Math. Series No. 55, edited by A. Abramowitz and I. A. Stegun, (U.S. GPO, Washington, D.C., 1964), Chap. 14, p. 538.
[32]S. Wolfram, *Mathematica, A System for Doing Mathematics by Computer* (Addison-Wesley, Reading, MA, 1988).
[33]R. J. Bell, W. T. Bousman, G. M. Goldman, and D. G. Rathbun, Surf. Sci. **7**, 293 (1967).
[34]Y. C. Lee and W. N. Mei, J. Phys. C **15**, L545 (1982).